Turkish Journal of Forecasting vol. 07 no. 1 (2023) pp. 01-09

Content list available at JournalPark

Turkish Journal of Forecasting

Journal Homepage: tjforecasting.com

# Improving Mass Detection in Mammography Using Focal Loss Based RetinaNet

S. Demirel[1,*], A. Urfali[1,2], O.F. Bozkir[1], A. Celikten[1,3], A. Budak[1], H. Karatas[1]

[1]*Akgun Computer Inc., Department of Artificial Intelligence and Image Processing, Ankara, Turkey*
[2]*Konya Technical University, Faculty of Engineering, Department of Computer Engineering, Konya, Turkey*
[2]*Ege University, Faculty of Engineering, Department of Computer Engineering, Izmir, Turkey*

A R T I C L E I N F O

*Article history*:

| | | | |
|---|---|---|---|
| Received | 12 | July | 2023 |
| Revision | 29 | August | 2023 |
| Accepted | 17 | October | 2023 |
| Available online | 20 | October | 2023 |

*Keywords*:
Breast Cancer
RetinaNet
Mass Detection
Focal Loss
Detectron2
Object Detection

R E S E A R C H A R T I C L E

A B S T R A C T

Breast cancer is a significant global health issue and plays a crucial role in improving patient outcomes through early detection. This study aims to enhance the accuracy and efficiency of breast cancer diagnosis by investigating the application of the RetinaNet and Faster R-CNN algorithms for mass detection in mammography images. A specialized dataset was created for mass detection from mammography images and validated by an expert radiologist. The dataset was trained using RetinaNet and Faster R-CNN, a state-of-the-art object detection model. The training and testing were conducted using the Detectron2 platform. To avoid overfitting during training, data augmentation techniques available in the Detectron2 platform were used. The model was tested using the AP50, precision, recall, and F1-Score metrics. The results of the study demonstrate the success of RetinaNet in mass detection. According to the obtained results, an AP50 value of 0.568 was achieved. The precision and recall performance metrics are 0.735 and 0.60 respectively. The F1-Score metric, which indicates the balance between precision and recall, obtained a value of 0.66. These results demonstrate that RetinaNet can be a potential tool for breast cancer screening and has the potential to provide accuracy and efficiency in breast cancer diagnosis. The trained RetinaNet model was integrated into existing PACS (Picture Archiving and Communication System) systems and made ready for use in healthcare centers.

Turkish Journal of Forecasting by Giresun University, Forecast Research Laboratory is licensed under a Creative Commons Attribution-ShareAlike 4.0 International License.

## 1. Introduction

Breast cancer occurs when a woman's breast cell divides abnormally and deteriorates [1]. Over time, the cancer cell spreads by damaging the breast tissues and cells. This condition can lead to encountering an irreversibly severe mass that cannot be treated. Mammography is among the most commonly used methods for the diagnosis of breast cancer [2].

Using mammography, a mass in the breast tissue can be detected as benign, allowing for early treatment. Due to the insufficient technology in developing countries, women are more affected by breast cancer [3]. Therefore, in recent years, emerging artificial intelligence technologies can be used to make healthcare services more efficient and accessible.

* Corresponding author.
*E-mail addresses*: semih.demirel@akgun.com.tr (Semih Demirel)

https://doi.org/10.34110/forecasting.1326245
2618-6594/© 2023 Turkish Journal of Forecasting. All rights reserved.

It is possible to draw a bounding box around the mass using CNN (Convolutional Neural Network)-based object detection models. In object detection models, features are extracted from images using the backbone network. Using these features, bounding box regression and object classification are performed [4]. Single-stage models, consisting of a single network, pass an input image through the network and perform localization and classification in the head layer [5]. The most important characteristic of two-stage models is the generation of anchors on regions likely to contain objects. Binary classification is performed on the generated anchors, distinguishing foreground and background, to eliminate the majority of negative anchors [6]. By performing bounding box regression and object classification on positive anchors, a final detection is achieved.

The fight against breast cancer holds critical importance for humanity. Therefore, in the literature, various results were obtained by using deep learning methods for combating breast cancer.

In the study conducted by [7], the impact of introducing a noise effect on image annotations during training was investigated. In the study, the quantitative evaluation of the performance of real bounding box coordinate noises was conducted on mammography images using Faster R-CNN (Faster Region-Based Convolutional Neural Network)[8]. It was noted that increasing the level of noise improved the object detection performance without increasing the model complexity.

The algorithm proposed by [9] suggests a diagnostic system by extracting mass features from breast images. The performance of the SVM (Support Vector Machine) model was enhanced by selecting parameters using the PSO (Particle Swarm Optimization) algorithm. Performance evaluation was carried out using the ROC (Receiver Operating Characteristic) metric, and an approximate ROC value of 0.96 was obtained.

In the study conducted by [10], an unsupervised method was used to detect masses. In the study, a hierarchical clustering method was used to perform regional feature extraction in order to reduce the false positive rate. A ROC value of 0.93 was obtained for normal and mass classification.

In their study [11], they experimented with hybrid methods to highlight the regions with a probability of containing a mass during mass segmentation. A mammography image was divided into two parts and segmented using an adaptive multi-thresholding method with the assistance of three different image segmentation techniques. The proposed method outperformed the compared models with an accuracy of 0.95 and achieved a specificity value of 0.97.

In their research, [12] uses the Digital Database for Screening Mammography (DDSM) collection to extract mammography images from those who were affected. This novel approach employing Federated Learning streamlines processing time and enhances model performance. Subsequently, feature extraction becomes paramount, with the adoption of the DenseNet [13] architecture. The extracted features are then channelled into the classification phase, bolstered by Enhanced Recurrent Neural Networks (E-RNN) for precise breast cancer detection. Simulation outcomes indicate a notable achievement, with the proposed method exhibiting 95% accuracy and 91% Matthews Correlation Coefficient (MCC).

As part of the study [14], BSNet used a dataset of 2321 multi-view mammography cases that were gathered from female individuals who underwent digital mammography at the Harbin Medical University Cancer Hospital. BSNet is a novel weakly supervised deep learning framework designed for non-invasive diagnosis of breast cancer with a focus on determining the hormone receptor (HR) status. Training and validation on this dataset demonstrated impressive results. Notably, BSNet achieved average Area Under the Curve (AUC) values of 0.89 and 0.92 on the test and external validation sets, respectively.

In the research conducted by [15], the study employs deep learning algorithms to process the wealth of information gathered from the multimodal images. Specifically, fusion classification models are utilized at both pixel and decision levels. This dual-pronged approach significantly enhances the accuracy and reliability of breast cancer diagnosis. The proposed method exhibits remarkable performance in breast cancer diagnosis. The Area Under the Curve (AUC) score, a key metric in diagnostic accuracy, attains an impressive 0.9366 for pixel fusion classification, with an associated accuracy of 89.01%.

In the research conducted by [16], a cascade network is implemented, combining a UNet [17] architecture for segmentation and a ResNet [18] backbone for classification. The segmentation process entails generating a mask that isolates the tumor from the image, enabling precise classification. The segmentation model, utilizing the UNet architecture, demonstrated a remarkable F1-score of 97.30%. The final decision-making layer of the cascade network

employs a straightforward 8-layer neural network, following the ResNet50 model. This classification framework exhibited a commendable accuracy rate of 98.61%, coupled with an impressive F1 score of 98.41%.

In their study, [19] proposed a system that integrates a radon transform, a data augmentation module, and a hybrid CNN architecture to achieve enhanced breast cancer detection. A mathematical morphological-based segmentation algorithm is utilized to precisely identify cancerous pixels. This step plays a pivotal role in accurately delineating the boundaries of cancer regions within abnormal mammogram images. The developed CNN architecture demonstrates impressive performance, achieving high sensitivity and specificity scores of 97.91% and 97.83%, respectively.

In the research study [20], a substantial mammography dataset was curated, encompassing 4,810 mammograms and comprising 6,663 microcalcification lesions, with biopsy results confirming 3,301 as malignant and 3,362 as benign. This comprehensive dataset formed the foundation for the development and testing of the automated system, drawing images from various medical centers. The automated deep-learning pipeline demonstrated commendable classification accuracy, with values of 0.8124 and 0.7237 for the training and test sets, respectively, in distinguishing between benign and malignant breasts.

In this study, mass detection was performed on mammography images using RetinaNet [21] and Faster R-CNN, an object detection models available in the Detectron2 platform. The following are the study's significant contributions:

- By enabling precise localization of suspicious lesions within mammograms, RetinaNet allows radiologists to concentrate on potential areas of concern.
- Its balanced approach in sensitivity and specificity is evident, effectively decreasing both false negatives and false positives in breast cancer detection.
- Integrated into PACS systems, RetinaNet offers a comprehensive diagnostic tool that merges automated detection with computer-assisted diagnosis.
- This research contributed to the development of annotated datasets, promoting further progress in this field and enabling the training of more accurate models.
- The ability of RetinaNet to detect early signs of breast cancer increases the chances of achieving successful treatment outcomes.

In the subsequent sections, we introduce the methodology in the second section. Detailed information about the dataset and the models used is provided. The third section discusses the results of the models. The fourth section contains the discussion. Finally, in the fifth section, we present the conclusion.

## 2. Materials and Methods

This section introduces the RetinaNet architecture, which consists of a single network, and the Focal Loss [21], a loss function that enhances object detection performance.

### 2.1. Dataset

In this study, mass detection was performed on mammography images using a private dataset obtained from Karadeniz Technical University. Ethical approval from the relevant institutional review board was obtained for the acquisition of the dataset. The dataset consists of a total of 3178 images. The dataset was divided into train, val, and test sets. Details about the dataset are provided in Table 1.

**Table 1.** Details of the dataset

| | **Train** | **Validation** | **Test** |
|---|---|---|---|
| Private Dataset | 2378 | 400 | 400 |

In Table 1, the number of train, validation, and test data is 2378, 400, and 400, respectively.

To prevent overfitting on the training data, data augmentation techniques available in the Detectron2 platform were used. These augmentation techniques include adjusting pixel value saturation, brightness, and contrast. Additionally, images were randomly rotated by a certain degree through rotation augmentation. Flip techniques were also applied to enhance the performance.

Sample images from the dataset are shown in Figure 1.

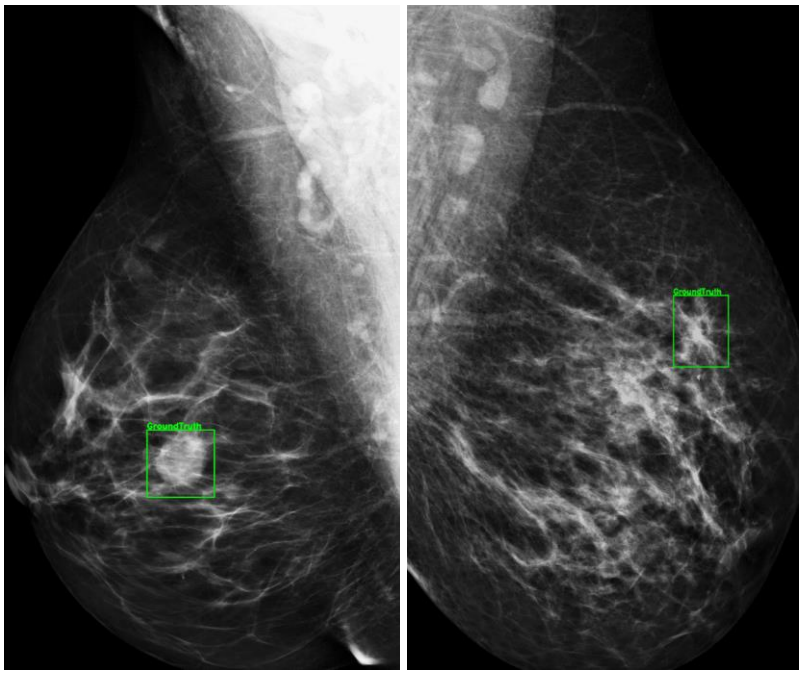


**Figure 1.** Sample annotated mammography images from the dataset

In Figure 1, the green boxes represent the actual bounding boxes indicating the masses.

### 2.2. RetinaNet

RetinaNet performs object detection by utilizing the outputs obtained from the backbone network to perform bounding box regression and classify the expected bounding boxes containing objects [22]. FPN (Feature Pyramid Network) [23] was integrated into the backbone network of RetinaNet, and features were extracted at different scales from single-size images. As the depth of the backbone increases and successive pooling and convolutional layers are applied, the spatial resolution decrease [24]. FPN extracts meaningful features from intermediate layers using the bottom-up pathway technique in a backbone network. The high-resolution features obtained from the top-down pathway are combined with the features from the bottom-up pathway to achieve spatial resolution [21]. Figure 2 presents the ResNet and FPN structure of the RetinaNet architecture.

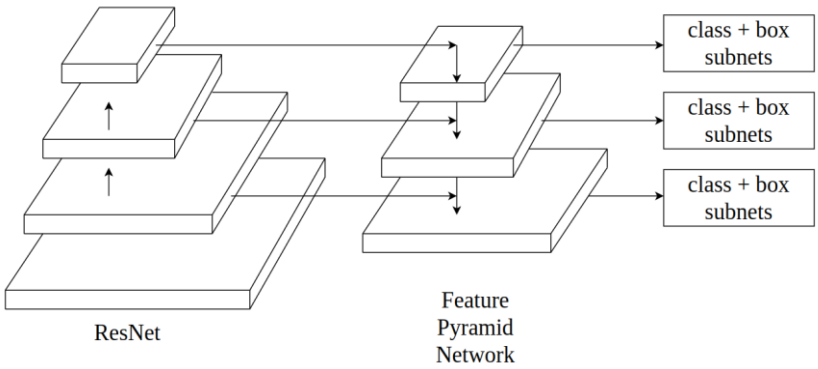


**Figure 2.** ResNet and FPN structure of the RetinaNet [21]

In Figure 2, a graphical representation illustrating the architectural components of the RetinaNet model is presented. The ResNet architecture was incorporated into the RetinaNet to empower the model with the capacity to learn intricate features and relationships within the data. The Feature Pyramid Network (FPN) complements the ResNet architecture by providing a multi-scale feature representation of the input data.

Class and box subnets are illustrated in Figure 3.

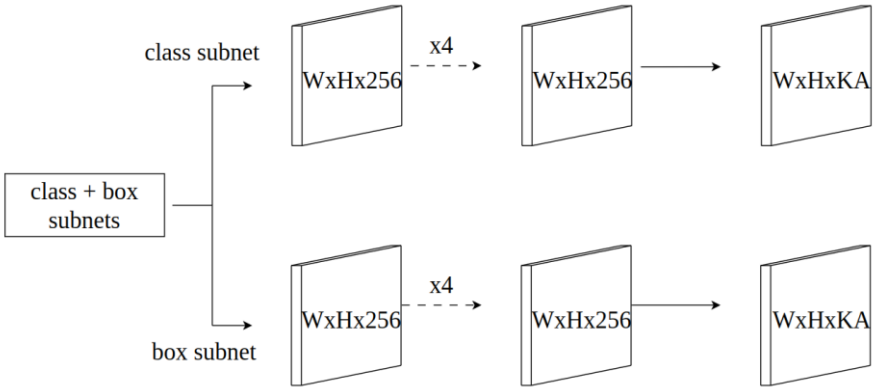


**Figure 3.** Class and box subnets of the RetinaNet architecture [21]

Figure 3 provides a visual representation depicting the complementary components of the RetinaNet architecture, focusing on the Class and Box subnets. W and H typically represent the width and height dimensions of the feature maps, respectively. K refers to the number of object classes and A denotes anchors [25]. The Class Subnet pertains to a critical aspect of object detection, namely, the classification of detected objects into distinct categories or classes. This component is responsible for assigning a probability distribution over the various classes to objects identified within an image [26]. Conversely, the Box Subnet is primarily concerned with the precise localization of detected objects. This component refines the bounding box coordinates that enclose the identified objects, effectively providing accurate spatial information about their positions within the image.

### 2.3. Focal Loss

Focal Loss was proposed with RetinaNet to address the imbalance issue in situations where there are many backgrounds and a small amount of foreground. To reduce the background effect, more weight is given to objects that are difficult to detect [24]. Focal Loss was developed by drawing inspiration from the commonly used Cross Entropy loss for binary classification problems [21]. Cross Entropy is a loss function that measures the similarities between the true label distribution and the predicted distribution. Equation 1 provides the Cross Entropy.

$$CE(p,y) = \begin{cases} -\log(p) if y = 1 \\ -\log(1-p) otherwise \end{cases} \quad (1)$$

where, $y$ represents the positive and negative binary true value, while $p$ represents the predicted probability.

The background, being the class majority and easily classified, negatively affects the gradients and hence the performance of cross entropy [21]. The class imbalance effect is addressed by integrating a factor into cross entropy. The integrated factor is provided in Equation 2.

$$(1-p_t)^{\gamma} \quad (2)$$

where, γ is denoted as the focusing parameter and is greater than or equal to 0. Focal Loss is given in Equation 3.

$$FL(p_t) = -(1-p_t)^{\gamma}\log(p_t) \quad (3)$$

where, $p_t$ represents the predicted probability value, and the focusing parameter given in Equation 2 is used for Focal Loss.

### 2.4. The Integration of the Model into PACS Systems

The purpose of the trained model is to perform mass detection in mammography images, providing an early diagnosis. In order for the model to serve as an artificial intelligence diagnostic system, it needs to be utilized in healthcare centers. Therefore, the trained model was integrated into existing PACS systems, making it a ready-to-use diagnostic tool.

## 3. Results

The training was conducted using RetinaNet available in the Detectron2 platform. After training, the model was tested using the images reserved for testing. The results were compared using the average precision metric.

Average precision is a metric used to measure performance in object detection and segmentation tasks. Average precision is a metric calculated by drawing a curve of precision and recall results at different IoU (Intersection over Union) threshold values [27]. The calculation of AP50 (Average Precision at 50) involves several steps. First, a Precision-Recall Curve is generated by obtaining precision and recall values at different threshold levels, typically ranging from 0 to 1. Next, the results of object detection are sorted based on these threshold values. Then, linear interpolation is applied to the Precision-Recall curve. This involves connecting adjacent points on the curve with straight lines to estimate the precision at %50 recall [27]. Finally, the area under the interpolated curve is computed using numerical integration methods. The mathematical expression of the AP50 metric is given in Equation 4.

$$AP50 = (1/N)\sum_{k=1}^{N}(P(k) * rel(k)) \tag{4}$$

where, *n* is the total number of items, *P(k)* is the precision at the $k^{th}$ position in the ranked list. *rel(k)* is an indicator function that is 1 if the item at position *k* is relevant, and 0 otherwise.

Precision measures the ratio of true positives to the total positive predictions. It represents the accuracy of positive predictions. Equation 5 provides the precision's mathematical expression.

$$precision = \frac{TP}{TP + FP} \tag{5}$$

Recall measures the ratio of true positives to the total actual positives. It represents the sensitivity of the model. Recall formula is given in Equation 6.

$$recall = \frac{TP}{TP + FN} \tag{6}$$

F1-score is a metric that balances precision and recall. Low values indicate an imbalance in precision or recall. Equation 7 gives the F1-score.

$$F1 - score = 2 \times \frac{precision \times recall}{precision + recall} \tag{7}$$

In this study, the performance of the RetinaNet and Faster R-CNN models were evaluated using the precision, recall, F1-score and AP50 metrics.

Table 2 presents the test results of RetinaNet and Faster R-CNN models.

**Table 2.** Test results of RetinaNet and Faster R-CNN

| **Model** | RetinaNet | RetinaNet | Faster R-CNN | Faster R-CNN |
|---|---|---|---|---|
| Backbone | ResNet101+FPN | ResNet50+FPN | ResNet101+FPN | ResNet101+FPN |
| Precision | 0.735 | 0.7664 | 0.6131 | 0.5735 |
| Recall | 0.60 | 0.4417 | 0.6552 | 0.6601 |
| F1-Score | 0.66 | 0.5604 | 0.6350 | 0.6137 |
| AP50 | 0.568 | 0.502 | 0.544 | 0.523 |

In Table 2, test results with different backbones for RetinaNet and Faster R-CNN models are provided. Feature extraction was performed using ResNet50 and ResNet101 backbones for the models, respectively. Additionally, FPN integration was provided for all backbones.

Table 3 provides details about the hyperparameters used for training RetinaNet and Faster R-CNN models.

**Table 3.** Hyperparameters of RetinaNet and Faster R-CNN models

| **Model** | Batch Size | Learning Rate | Iteration | Solver Step | Loss |
|---|---|---|---|---|---|
| RetinaNet | 16 | 0.001 | 24000 | 18000 | Focal Loss |
| Faster R-CNN | 16 | 0.001 | 24000 | 18000 | Cross Entropy |

Table 3 provides the hyperparameters used during the training of RetinaNet and Faster R-CNN models. The model's performance was improved by using a batch size of 16. A learning rate of 0.001 was employed to facilitate the convergence of gradients in earlier iterations. The models were trained for 24,000 iterations, with a learning rate decay of 0.1 at 18,000 iterations. The loss functions of the RetinaNet and Faster R-CNN models are focal loss and cross entropy, respectively.

## 4. Discussion

The RetinaNet architecture with a ResNet101 backbone and Feature Pyramid Network (FPN), demonstrates a high level of precision (73.5%), indicating that when it predicts an object, it is correct around 73.5% of the time. The recall of 60% signifies that it effectively captures 60% of the actual objects in the dataset. The F1-Score of 66% is a balanced measure that considers both precision and recall. The AP50 of 56.8% is a specialized metric evaluating the precision of object localization at an Intersection over Union (IoU) threshold of 50%.

The RetinaNet model, employing a ResNet50 backbone with FPN, exhibits high precision at 76.64%, suggesting accurate predictions. However, it shows lower recall at 44.17%, indicating it misses a significant portion of actual objects. The F1-Score of 56.04% represents a trade-off between precision and recall. The AP50 score of 50.2% suggests that the model performs moderately well in terms of object localization.

The Faster R-CNN model, utilizing a ResNet101 backbone with FPN, displays precision of 61.31%, indicating relatively accurate object predictions. The recall of 65.52% suggests that it captures a substantial portion of actual objects. The F1-Score of 63.50% signifies a balanced performance in terms of precision and recall. The AP50 score of 54.4% demonstrates a good ability to localize objects.

The Faster R-CNN model, based on a ResNet50 backbone with FPN, shows precision at 57.35%, indicating reasonable accuracy in object predictions. A recall of 66.01% suggests it captures a significant proportion of actual objects. The F1-Score of 61.37% represents a balanced performance between precision and recall. The AP50 score of 52.3% indicates a moderate ability to localize objects.

Among the evaluated object detection models, the RetinaNet with ResNet101+FPN architecture emerged as the top performer in terms of F1-Score, achieving an impressive score of 66%. This model demonstrated a commendable balance between precision (73.5%) and recall (60%), indicating a high level of accuracy in its predictions while effectively capturing a substantial portion of actual objects. These results suggest that for tasks where a harmonious blend of precision and recall is critical, the RetinaNet with ResNet101+FPN model stands out as the most suitable choice.

RetinaNet outperforms Faster R-CNN primarily due to its innovative use of the Focal Loss. Unlike the standard Cross Entropy Loss used in Faster R-CNN, the Focal Loss dynamically adjusts the weight assigned to each training example based on its classification difficulty. This means that RetinaNet places greater emphasis on learning from challenging instances, which is especially beneficial in scenarios with imbalanced class distributions. This approach results in a more robust and precise object detector, ultimately leading to superior performance compared to Faster R-CNN, especially in scenarios with complex backgrounds or a high degree of class imbalance.

Figure 4 displays sample images of the RetinaNet with ResNet101+FPN results.

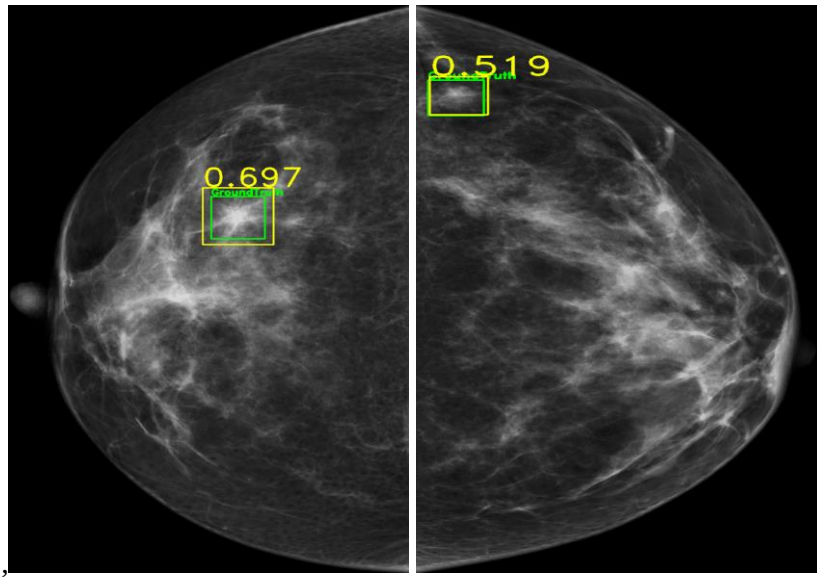


**Figure 4.** Sample images for the detection results of the RetinaNet with ResNet101+FPN model

In Figure 4, the green and yellow colors respectively represent the ground truth bounding box and the predicted bounding box for the mass. The predicted boxes also display confidence score values.

## 5. Conclusion

In this study, we applied two state-of-the-art object detection models, RetinaNet and Faster R-CNN, for mass detection on mammography images. The RetinaNet with ResNet101+FPN demonstrated exceptional performance, achieving a precision of 73.5%, recall of 60%, and an F1-score of 66%. This model exhibited a commendable balance between precision and recall and demonstrated a high ability to localize objects with an AP50 score of 56.8%. These findings suggest that RetinaNet with ResNet101+FPN can serve as valuable tools in computer-aided diagnostic systems for breast cancer screening. The successful integration of these models into PACS systems and their transformation into intelligent diagnostic systems further underlines their potential impact in clinical practice, representing a significant advancement in breast cancer diagnostic technology.

Future studies could explore integrating multi-modal imaging data, employing advanced pre-processing techniques, and investigating state-of-the-art deep learning architectures. Conducting larger-scale studies in real-world clinical settings and incorporating explainability techniques are crucial steps to further enhance the application of object detection models in breast cancer diagnosis. These endeavors hold significant potential for improving patient outcomes in the field of computer-aided breast cancer diagnosis.

## Acknowledgments

This study was supported by AKGUN Computer Incorporated Company. We would like to thank Akgun Computer Inc. for providing all the necessary resources and funding for the execution of this study.

## References

[1] K. Loizidou, R. Elia, C. Pitris, Computer-aided breast cancer detection and classification in mammography: A comprehensive review, Computers in Biology and Medicine. 153 (2023) 106554. doi:https://doi.org/10.1016/j.compbiomed.2023.106554

[2] S.J. Frank, A deep learning architecture with an object-detection algorithm and a convolutional neural network for breast mass detection and visualization, Healthcare Analysis. 3 (2023) 100186. doi:https://doi.org/10.1016/j.health.2023.100186

[3] J. Bai, R. Posner, T. Wang, C. Yang, S. Nabavi, Applying deep learning in digital breast tomosynthesis for automatic breast cancer detection: A review, Medical Image Analysis. 71 (2021) 102049. doi:https://doi.org/10.1016/j.media.2021.102049

[4] L. Abdelrahman, M.A. Ghamdi, F.C. Mesa, M.A. Mottaleb, Convolutional neural networks for breast cancer detection in mammography: A survey, Computers in Biology and Medicine. 131 (2021) 104248. doi:https://doi.org/10.1016/j.compbiomed.2021.104248

[5] L. Garrucho, K. Kushibar, S. Jouide, O. Diaz, L. Igual, K. Lekadir, Domain generalization in deep learning based mass detection in mammography: A large-scale multi-center study, Artificial Intelligence in Medicine. 132 (2022) 102386. doi:https://doi.org/10.1016/j.artmed.2022.102386

[6] A. Baccouche, B.G. Zapirain, Y. Zheng, A.S. Elmaghraby, Early detection and classification of abnormality in prior mammograms using image-to-image translation and YOLO techniques, Computer Methods and Programs in Biomedicine. 221 (2022) 106884. doi:https://doi.org/10.1016/j.cmpb.2022.106884

[7] S. Famouri, L. Morra, L. Mangia, F. Lamberti, Breast mass detection with faster r-cnn: On the feasibility of learning from noisy annotations, IEEE Access. 9 (2021) 66163-66175. doi:10.1109/ACCESS.2021.3072997

[8] S. Ren, K. He, R. Girshick, J. Sun, Faster R-CNN: Towards real-time object detection with region proposal networks, IEEE Transactions on Pattern Analysis and Machine Intelligence. 39 (2016) 1137-1149. doi:10.1109/TPAMI.2016.2577031

[9] M. W. A. El-Soud, I. Zyout, K. M. Hosny, M. M. Eltoukhy, Fusion of orthogonal moment features for mammographic mass detection and diagnosis, IEEE Access. 8 (2020) 129911-129923. doi:10.1109/ACCESS.2020.3008038

[10] S. Imran, B. A. Lodhi, A. Alzahrani, Unsupervised method to localize masses in mammograms, IEEE Access. 9 (2021) 99327-99338. doi:10.1109/ACCESS.2021.3094768

[11] G. Toz, P. Erdoğmuş, A novel hybrid image segmentation method for detection of suspicious regions in mammograms based on adaptive multi-thresholding (HCOW), IEEE Access. 9 (2021) 85377-85391. doi:10.1109/ACCESS.2021.3089077

[12] S. Kumbhare, A.B. Kathole, and S. Shinde, Federated-learning aided breast cancer detection with intelligent heuristic-based deep learning framework, Biomedical Signal Processing and Control. 86 (2023) 105080. doi: https://doi.org/10.1016/j.bspc.2023.105080

[13] G. Huang, Z. Liu, L.V.D. Maaten, K.Q. Weinberger, Densely connected convolutional networks, in: 2017 IEEE Conference on Computer Vision and Pattern Recognition (CVPR), 2017: pp. 2261-2269. doi: 10.1109/CVPR.2017.243

[14] M. Zhang, C. Wang, L. Cai, J. Zhao, Y. Xu, J. Xing, J. Sun, Y. Zhang, Developing a weakly supervised deep learning framework for breast cancer diagnosis with HR status based on mammography images, Computational and Structural Biotechnology Journal. 22 (2023) 17-36. doi: https://doi.org/10.1016/j.csbj.2023.08.012

[15] J. Wu, Z. Xu, L. Shang, Z. Wang, S. Zhou, H. Shang, H. Wang, J. Yin, Multimodal microscopic imaging with deep learning for highly effective diagnosis of breast cancer, Optics and Lasers in Engineering. 168 (2023) 107667. doi: https://doi.org/10.1016/j.optlaseng.2023.107667

[16] B. Asadi, Q. Memon, Efficient breast cancer detection via cascade deep learning network, International Journal of Intelligent Networks. 4 (2023) 46-52. doi: https://doi.org/10.1016/j.ijin.2023.02.001

[17] O. Ronneberger, P. Fischer, T. Brox, U-Net Convolutional Networks for Biomedical Image Segmentation, in: Medical Image Computing and Computer-Assisted Intervention MICCAI 2015, 2015: pp. 234-241. doi: https://doi.org/10.1007/978-3-319-24574-4_28

[18] K. He, X. Zhang, S. Ren, J. Sun, Deep residual learning for image recognition, in: 2016 IEEE Conference on Computer Vision and Pattern Recognition (CVPR), 2016: pp. 770-778. doi:10.1109/CVPR.2016.90

[19] R. S. Raaj, Breast cancer detection and diagnosis using hybrid deep learning architecture, Biomedical Signal Processing and Control. 82 (2023) 104558. doi: https://doi.org/10.1016/j.bspc.2022.104558

[20] Q. Lin, W.M. Tan, J.Y. Ge, Y. Huang, Q. Xiao, Y.Y. Xu, Y.T. Jin, Z.M. Shao, Y.J. Gu, B. Yan, K.D. Yu, Artificial intelligence-based diagnosis of breast cancer by mammography microcalcification, Fundamental Research. (2023).

[21] T. Y. Lin, P. Goyal, R. Girshick, K. He, P. Dollar, Focal loss for dense object detection, in: 2017 IEEE International Conference on Computer Vision (ICCV), 2017: pp. 2999-3007. doi:10.1109/TPAMI.2018.2858826

[22] G. Hamed, M. Marey, S. E. Amin, M. F. Tolba, Automated breast cancer detection and classification in full field digital mammograms using two full and cropped detection paths approach, IEEE Access. 9 (2021) 116898-116913. doi:10.1109/ACCESS.2021.3105924

[23] T. Y. Lin, P. Dollar, R. Girshick, K. He, B. Hariharan, S. Belongie, Feature pyramid networks for object detection, in: 2017 IEEE Conference on Computer Vision and Pattern Recognition (CVPR), 2017: pp. 936-944. doi:10.1109/CVPR.2017.106

[24] T. Miao, H. Zeng, W. Yang, B. Chu, F. Zou, W. Ren, J. Chen, An improved lightweight retinanet for ship detection in SAR images, IEEE Journal of Selected Topics in Applied Earth Observations and Remote Sensing. 15 (2022) 4667-4679. doi:10.1109/JSTARS.2022.3180159

[25] J. Liu, R. Jia, W. Li, F. Ma, H.M. Abdullah, H.Ma, M.A. Mohamed, High precision detection algorithm based on improved RetinaNet for defect recognition of transmission lines, Energy Reports. 6 (2020) 2430-2440. doi: https://doi.org/10.1016/j.egyr.2020.09.002

[26] H. Peng, Z. Li, Z. Zhou, Y. Shao, Weed detection in paddy field using an improved RetinaNet network, Computers and Electronics in Agriculture. 199 (2022) 107179. doi: https://doi.org/10.1016/j.compag.2022.107179

[27] R. Viola, L. Gautheron, A. Habrard, M. Sebban, MetaAP: A meta-tree-based ranking algorithm optimizing the average precision from imbalanced data, Pattern Recognition Letters. 161 (2022) 161-167. doi: https://doi.org/10.1016/j.patrec.2022.07.019